Received Least Squares Beamforming on Ka-band Channel Model of HAP System

Irma Zakia, Suhartono Tjondronegoro, Iskandar, and Adit Kurniawan

School of Electrical Engineering and Informatics, Institut Teknologi Bandung,
Jl. Ganesha no. 10, Bandung 40132, Indonesia
irma.zakia@students.itb.ac.id, shtntjnegoro@stei.itb.ac.id,
iskandar@stei.itb.ac.id, adit@stei.itb.ac.id

Abstract: The Ka-band channel model ofHigh Altitude Platform (HAP) for high speed train is modeled as a flat and time varying Rician process with 10-25 dB Rician factor. In order to compensate for the time varying fading channel and considering the fact that the Line-of-Sight (LOS) component is dominant, adaptive beamforming with the least-squares (LS) approach is employed at the receiver. Theoretical analysis of the LS algorithm is performed for very large Rician factor in the high Signal to Noise Ratio (SNR) regime. In particular, the analysis is with respect to the estimated autocorrelation matrix of the received vector and the beamforming weight. It is shown that, the estimated autocorrelation matrix of the received vector resembles the autocorrelation matrix of the array steering response. The presented analysis are then verified by Monte Carlo simulations.

Keywords: least-squares (LS), High Altitude Platform (HAP), Ka-band, beamforming, doppler

1. Introduction

As the high requirement for wireless services is inevitable, solutions for developing another wireless platform has risen. One of the services which has attracted extensive work and research recently is the requirement of providing data connections on high speed trains from existing platforms [1][2][3] as well as the emerging HAP [4][5].

Existing internet connectivity on high speed trains is given by a combination [5] of terrestrial, like UMTS, WiMAX [3], and satellite platforms. If LOS link is available, satellite system is employed in order to achieve high data rates, whereas when the train travels into deep tunnels, terrestrial system is provided to render the possibility of connectivity loss to a minimum. Accordingly, the data rate is influenced by satellite performance, which is limited to 2 Mbps [6]. In contrast, the emerging HAP platform aims at the delivery of up to 120 Mbps data rate for trains travelling until 300 kmph, under the CAPANINA project [4][7]. Furthermore, HAP serves high speed train with lower infrastructure cost if compared to the existing terrestrial railway communication, thanks to its possible 200 km diameter coverage. If compared to a 36000 km orbiting satellite, delay propagation is of no issue on HAP.

The frequency operation of the downlink from HAP to high speed trains is Ka-band. The channel in this band is mainly LOS, whereas the nonLOS (NLOS) channel component which reflects the short-term fading, is modeled by at most two rays, each originating from different cluster [7]. In this paper, it is assumed that the railways are mostly located in rural areas. This yields the channel model consisting of a LOS link and a single ray with time indifferentiable path w.r.t. the LOS [7]. Overall, the channel is flat with Rician distributed envelope.

Since the vehicle involved is moving with high speed, a major problem is the dopplereffect which creates a time varying channel.In rural areas, moderate to high Rician factor is assumed [7], thus the received signal is mainly concerned with doppler shift which translates to a rotation of the received signal constellation. Nevertheless, if thisdoppler shifted signal is left uncompensated, a worst Bit Error Rate (BER) results [4][8].

Received: October 8th, 2013. Accepted: December 21st, 2013

If thedoppler shift isestimated [9][10][11], the channel mean becomes adeterministic constant parameter. Hence, the time-varying channel can be compensated by existing schemes which operate on Rician channel with constant mean, such as [12][13].But these schemes then depend on the doppler shift estimator performance. Besides, the channel is not only affected bydoppler shift, but also doppler spread for lower Rician factor[14]. The estimation of simply the doppler shift is insufficient, thus, tracking the time varying channel is required.

The physical layer adopted in this research resembles the IEEE 802.16 single carrier for Fixed Wireless Access (FWA) as proposed in [4]. This yields the channel as slow fading. With the slow fading assumption, tracking the time varying channel can be accomplished by adaptive filters, one of which is adaptive filter with the LS approach [4]. In particular, the filter is implemented in spatial domain by forming antenna arrays at the receiver. This results in LS beamforming, for which the implementation is carried out as recursive LS (RLS). The tracking is performed on the Decision Directed (DD) mode, after an initial convergence is achieved on the Data Aided (DA) one.

The contribution of this paper is on thetheoretical analysis of theLS algorithm for theKa-band channel model specified in [7].Specifically, the estimated received vector autocorrelation matrix and the beam forming weight analysis are carried out in the high SNR regime for very large Rican factor. It is shown that, the estimated autocorrelation matrix of the received vector resembles the autocorrelation matrix of the array steering. Moreover, it is revealed that the beam forming weight is proportional to the array steering response, yet influenced by the Doppler effect due to the train velocity. The presented analysis are then verified by Monte Carlo simulations.

The rest of thepaper is organized as follows. Section 2 describes the transmission systems, whichcomprises the channel model and the transceiver structure. In Section 3, the LS beamforming algorithm as well as the theoretical analysis of the resulting beamf orming weight for very large Ricianfactor in the high SNR regime are presented. Afterwards, Section 4 deals with the time domain channel magnitude, estimated autocorrelation matrix of the received vector, and the beam forming weight power response obtained from Monte Carlo simulations. Furthermore, agreements of thelast two parameters to the theoretical analysis are shown. Finally, Section 5 concludes the paper and suggests topic for further investigations.

2. Transmission Systems

The transmission systems comprise the channel model and the transceiver structure. The channel model is already specified in [7] but a simplified model is adopted here. The transceiver structure resembles the IEEE 802.16 FWA physical layer [4].

In this paper, the transmission is the downlink from HAP equipped with a single antenna to an onboard receiver which is equipped with *N* antennas. The onboard receiver is assumed to be deployed on top of the carriage. The transmission systems between the onboard receiver and passengers inside the train are out of the research scope.

A. Channel Model

Before representing the simplified Ka-band channel model, it is important to note that the model considered is the short-term fading channel. Only a brief description considering the simplified Ka-band channel model is given here, whereas detail analysis can be found in [7]. The simplification is w.r.t. the number of antennas on HAP, which is a single one. Therefore, it is seen as Single Input Multiple Output (SIMO) communication, a special channel model case of [7].

By assumption, the train travels mainly over rural areas. This yields a single ray NLOS model, or in addition to the LOS component, the channel model is written as

$$\boldsymbol{h}(t) = \sqrt{\frac{K_R}{K_R+1}}\,\boldsymbol{h}_{LOS}(t) + \sqrt{\frac{1}{K_R+1}}\,\boldsymbol{h}_{NLOS}(t) \qquad (1)$$

frequency simply acts as reference, since physically, the HAP coverage is defined for $10^{\circ} \leq \psi_0 \leq 170^{\circ}$.

A.2. NLOS Component

By the assumption that the train travels mainly on rural areas, the NLOS component is modeled as a single ray which results in a flat fading channel [7]. The scaterrers in the atmosphere produces angle spread, whereas local scaterrers surrounding the terminal induces doppler spread. The statistical description of the NLOS component is represented by the time-spatial autocorrelation matrix

$$\boldsymbol{R}(\Delta t) = E\{\boldsymbol{h}_{NLOS}(t)\boldsymbol{h}_{NLOS}^{H}(t-\Delta t)\} \in \mathbb{C}^{\boldsymbol{N,N}} \quad (5)$$

where$E\{.\}$ denotes expectation. The matrix $\boldsymbol{R}(\Delta t)$ depends on the time difference Δt since $\boldsymbol{h}_{NLOS}(t)$ is assumed WSS.

Following the statistical independence assumption between the doppler angle of NLOS component ψ and its respective DOA θ, (5) becomes

$$\boldsymbol{R}(\Delta t) = R_{TD}(\Delta t)\boldsymbol{R}_{SD} \quad (6)$$

where$R_{TD}(\Delta t)$ refers to stochastic time autocorrelation for time difference Δt and$\boldsymbol{R}_{SD}$ is the stochastic spatial autocorrelation matrix. By definition,

$$R_{TD}(\Delta t) = E\{h_{NLOS;k}(t)h_{NLOS;k}^{*}(t-\Delta t)\} \quad \forall\, k, k = 1,2,..,N \quad (7)$$

where$h_{NLOS;k}(t)$ specifies the NLOS channel $\boldsymbol{h}_{NLOS}(t)$ for the k^{th} antenna. Due to the statistical independence assumption of $\psi$and θ, it is noted in (7) that $R_{TD}(\Delta t)$ is identical for all antennas, and hence a scalar. The employed time domain autocorrelation follows Clarks model [16]

$$R_{TD}(\Delta t) = J_0(2\pi F_D \Delta t) \quad (8)$$

Since the transmitter is assumed to have a single antenna, the transmitter steering response is 1, thus $\boldsymbol{R}_{SD}$ is defined as [7]

$$\boldsymbol{R}_{SD} = \int_{D(\theta)} \boldsymbol{a}_{RX}(\theta)\boldsymbol{a}_{RX}^{H}(\theta)p(\theta)d\theta \in \mathbb{C}^{\boldsymbol{N,N}} \quad (9)$$

The matrix $\boldsymbol{R}_{SD}$ has the following physical meaning. The $(k,l)^{\text{th}}$ element of$\boldsymbol{R}_{SD}$, with $k, l = 1,2,\ldots,N$, denotes NLOS correlation between the k^{th} and l^{th} pair. Each pair is regarded as the channel from one transmit to one received antenna. As the transmitter has single antenna, the k^{th} and l^{th} pairs express the channel from transmitter to received antenna k and l respectively.

The term $p(\theta)$ is the Probability Density Function (PDF) of the DOA θ. The DOA angle spread is affected by atmospheric conditions and is assumed to follow Gaussian distribution [7]

$$p(\theta) = \frac{1}{2\pi\sqrt{\sigma_\theta^2}} e^{\frac{-(\theta-\theta_0)^2}{2\sigma_\theta^2}} \quad (10)$$

where $\theta_0$and σ_θ^2 denotes the DOA mean and variance respectively. The higher the variance, the channel becomes less correlated spatially. Further details on the time-spatial autocorrelation matrix of the HAP Ka-band channel is found in [7][8].

Additionally, the beamforming gain can be calculated [17]

$$G_{BF} = \frac{SNR_{array}}{SNR_{elem}} \tag{13}$$

whereSNR_{array} is the resulting SNR at the beamformer output. From Figure 2, the beamformer output is expressed as

$$\boldsymbol{y}^T(n)\boldsymbol{w}(n) = (\boldsymbol{h}(n)x(n) + \boldsymbol{v}(n))^T\boldsymbol{w}(n) \tag{14}$$

where $\boldsymbol{w}[n] = [w_1[n]w_2[n] \dots w_N[n]]^T$ is the beamforming vector.

It follows that

$$SNR_{array} = \frac{E\{\|x(n)\boldsymbol{h}^T(n)\boldsymbol{w}(n)\|^2\}}{E\{\|\boldsymbol{v}^T(n)\boldsymbol{w}(n)\boldsymbol{w}^H(n)\boldsymbol{v}^*(n)\|^2\}} = \frac{E\{\boldsymbol{w}^H(n)\boldsymbol{h}^*(n)\boldsymbol{h}^T(n)\boldsymbol{w}(n)\}}{\sigma_v^2 E\{\boldsymbol{w}^H(n)\boldsymbol{w}(n)\}} \tag{15}$$

where the last equality assumes statistical independence between $\boldsymbol{v}(n)$ and $\boldsymbol{w}(n)$. Using (12), the beamforming gain becomes

$$G_{BF} = \frac{E\{\boldsymbol{w}^H(n)\boldsymbol{h}^*(n)\boldsymbol{h}^T(n)\boldsymbol{w}(n)\}}{E\{\boldsymbol{w}^H(n)\boldsymbol{w}(n)\}} \tag{16}$$

At the receiver, the channel is compensated by means of RLS adaptive beamforming. Afterwards, the transmitted data symbol are detected $\hat{x}[n]$.

From the receiver prespective, the receiver switches from DA to DD mode, and vice versa, as seen in Figure 2 and 3. Accordingly, the output of the symbol detector required for filtering is only in DD mode. The details on beamforming weight tracking $\boldsymbol{w}[n]$ is presented in Section 3.

3. Adaptive Least-squares Beamforming

A. Algorithm

By assuming the channel is dominant by the LOS component, [4] proposed received beamforming, where the time varying beamforming vector $\boldsymbol{w}[n]$ is tracked by the LS algorithm. Determining the vector $\boldsymbol{w}[n]$ is pursued by minimizing the cost function [15]

$$\mathcal{E}[n] = \sum_{i=1}^{n} \gamma^{n-i}\|e[i]\|^2 \tag{17}$$

where γ indicates the forgetting factor, $0 < \gamma < 1$ and $e[i]$ is the error at time $i = 1,2, \dots, n$. Before describing further, we would like to stress the fact that the LS algorithm incorporates the error $e[i]$ from time $i = 1$ to n. Therefore, n is referred as the most recent time index. Stacking the tracking error $e[i]$ from$i = 1$ to n in one column results in the error vector

$$\boldsymbol{\epsilon}[n] = [e[1], e[2], \dots e[n]]^T \in \mathbb{C}^{n,1} \tag{18}$$

As a consequence, (17) is rewritten as

$$\mathcal{E}[n] = \boldsymbol{\epsilon}^H[n]\,\boldsymbol{\Lambda}\boldsymbol{\epsilon}[n] \tag{19}$$

where$\boldsymbol{\Lambda} = \begin{pmatrix} \gamma^{n-1} & \cdots & 0 \\ \vdots & \ddots & \vdots \\ 0 & \cdots & 1 \end{pmatrix}$ is a diagonal matrix with exponentially forgetting factor on its diagonal elements. Furthermore, the error vector $\boldsymbol{\epsilon}[n]$is defined as

From the point of view of filtering, the elements of $\boldsymbol{w}[n]$ acts as the filter coefficients. The filter can be implemented in the spatial domainand executed on a single snapshot, or implemented within a tapped delay line structure (time domain implementation) which works on multiple snapshots. Since the the filter considered here is implemented in the spatial domain, the resulting correlation estimates ($\widehat{\boldsymbol{R}}_{\boldsymbol{yy}}$ and $\hat{\boldsymbol{r}}_{\boldsymbol{yx}}$) are correlation among different spatial antennas, not for different time..

If the filtering operation is implemented in time domain, then (22) has a completely different form [13]. In this case, (28) and (29) becomes the estimated time domain autocorrelation matrix and estimated time domain cross correlation vector respectively. Regardless of the fact that the filter weight can be implemented in spatial or time domain, the estimated autocorrelation matrix and cross correlation vector yet stem from time averaging.

B. Theoretical Analysis

The discrete-time channel model ($t = nT_s$) of (1) is expressed as

$$\boldsymbol{h}[n] = \sqrt{\frac{K_R}{K_R+1}}\boldsymbol{h}_{LOS}[n] + \sqrt{\frac{1}{K_R+1}}\boldsymbol{h}_{NLOS}[n] \tag{31}$$

Likewise to the fading channel $\boldsymbol{h}[n]$, the discrete-time LOS channel component is indicated by $\boldsymbol{h}_{LOS}[n] = \left[h_{LOS;1}[n], h_{LOS;2}[n], \dots, h_{LOS;N}[n]\right]^T$ and its NLOS component is represented by $\boldsymbol{h}_{NLOS}[n] = \left[h_{NLOS;1}[n], h_{NLOS;2}[n], \dots, h_{NLOS;N}[n]\right]^T$.

The remaining subsection belongs to the theoretical analysis of the impact of the LS beam forming weight on the Ka-band channel. Before proceeding to the analysis, we require the transposed of the column-wise vector $\boldsymbol{h}[i]$ concatenation from $i = 1$ to n. This yields

$$\boldsymbol{\mathcal{H}}[n] = [\boldsymbol{h}[1] \quad \boldsymbol{h}[2] \quad \dots \quad \boldsymbol{h}[n]]^T \in \mathbb{C}^{n,N} \tag{32}$$

In general, (31) is regarded as

$$\boldsymbol{h}[i] = \sqrt{\frac{K_R}{K_R+1}}\boldsymbol{h}_{LOS}[i] + \sqrt{\frac{1}{K_R+1}}\boldsymbol{h}_{NLOS}[i] \quad i = 1,2,\dots,n \tag{33}$$

Then, it follows that (32)yields

$$\boldsymbol{\mathcal{H}}[n] = \sqrt{\frac{K_R}{K_R+1}}\boldsymbol{\mathcal{H}}_{LOS}[n] + \sqrt{\frac{1}{K_R+1}}\boldsymbol{\mathcal{H}}_{NLOS}[n] \tag{34}$$

where

$$\boldsymbol{\mathcal{H}}_{LOS}[n] = [\boldsymbol{h}_{LOS}[1] \quad \boldsymbol{h}_{LOS}[2] \quad \dots \quad \boldsymbol{h}_{LOS}[n]]^T \in \mathbb{C}^{n,N} \tag{35}$$

and

$$\boldsymbol{\mathcal{H}}_{NLOS}[n] = [\boldsymbol{h}_{NLOS}[1] \quad \boldsymbol{h}_{NLOS}[2] \quad \dots \quad \boldsymbol{h}_{NLOS}[n]]^T \in \mathbb{C}^{n,N} \tag{36}$$

Using (34), the received signal matrix of (22) becomes

$$\boldsymbol{\mathcal{Y}}[n] = \text{diag}(\boldsymbol{\chi}[n])\boldsymbol{\mathcal{H}}[n] + \boldsymbol{\mathcal{V}}[n] \tag{37}$$

where

There are two conditions that require analysis. Firstly, if the mobile is static, i.e. $F_D = 0$. Looking at (44) and (45), the beam forming weight attempts to compensate perfectly for the received steering response

$$\boldsymbol{w}[n] \propto \boldsymbol{a}_{RX}^{*}(\theta_0) \tag{46}$$

The beam forming weight is required to track the DOA of the received signal. In this case, the beam forming weight is equivalent to a spatial matched filter which maximizes the output SNR [17].

Secondly, for moving mobile,$F_D \neq 0$, the beamforming weight immediately yields

$$\boldsymbol{w}[n] \propto \boldsymbol{a}_{RX}^{*}(\theta_0) \sum_{i=1}^{n} \gamma^{n-i}\, e^{-j2\pi F_D cos(\psi_0) i T_s} \tag{47}$$

Hence, besides tracking DOA, the beam forming weight requires to adjust its coefficients to the Doppler. In the CAPANINA scenario, the sampling rate $\frac{1}{T_s} = 20$ MHz, thus $F_D T_s = 0.00043$ for a train travelling speed of 300 kmph [4]. If each frame consists of 100 symbols, $e^{-j2\pi F_D cos(\psi_0) i T_s}$ in (47) can be considered constant for any $i = 1,2,..n$. In this case, it can be stated that

$$\boldsymbol{w}[n] \propto \boldsymbol{a}_{RX}^{*}(\theta_0) e^{-j2\pi F_D cos(\psi_0) n T_s} = \boldsymbol{h}_{LOS}^{*}[n] \tag{48}$$

Despite the fact that the Rician factor is very large (LOS dominant), it can be concluded that adaptive filtering is required at the receiver to track the time varying channel due to DOA and doppler shift.

B.2. Very Small Rician Factor

If Rician factor K_R is very small, then the channel

$$\boldsymbol{\mathcal{H}}[n] \approx \boldsymbol{\mathcal{H}}_{NLOS}[n],$$

which results in the received signal matrix

$$\boldsymbol{\mathcal{Y}}[n] \approx \text{diag}(\boldsymbol{\chi}[n])\boldsymbol{\mathcal{H}}_{NLOS}[n] + \boldsymbol{\mathcal{V}}(n) \tag{49}$$

In a similar fashion to the very large K_R case, it is observed here that in the high SNR regime

$$\widehat{\boldsymbol{R}}_{\boldsymbol{yy}} = \boldsymbol{\mathcal{H}}_{NLOS}^{H}[n]\text{diag}(\boldsymbol{\chi}^{\boldsymbol{H}}[n])\boldsymbol{\Lambda}\text{diag}(\boldsymbol{\chi}[n])\boldsymbol{\mathcal{H}}_{NLOS}[n] \tag{50}$$

For PSK symbols, as also considers in our research, $\text{diag}(\boldsymbol{\chi}^{\boldsymbol{H}}[n])\text{diag}(\boldsymbol{\chi}[n]) = \boldsymbol{I}_{\boldsymbol{n}}$, where $\boldsymbol{I}_{\boldsymbol{n}}$is a identity matrix with dimension n. Hence, by the nature of time-averaging in LS, (50) leads to

$$\widehat{\boldsymbol{R}}_{\boldsymbol{yy}} \propto E\{\boldsymbol{h}_{NLOS}[i]\boldsymbol{h}_{NLOS}^{H}[i]\} \text{for any } i = 1,2,..,n \tag{51}$$

Since $\boldsymbol{h}_{NLOS}[i]$ is a stochastic process, it is observed that for very small rician factor,$\widehat{\boldsymbol{R}}_{\boldsymbol{yy}}$ is similar to thestochastic spatial auto correlation matrix (9) or mathematically

$$\widehat{\boldsymbol{R}}_{\boldsymbol{yy}} \propto \boldsymbol{R}_{SD} \tag{52}$$

The crosscorrelation vector emerges from

A.2. Moderate Rician Factor

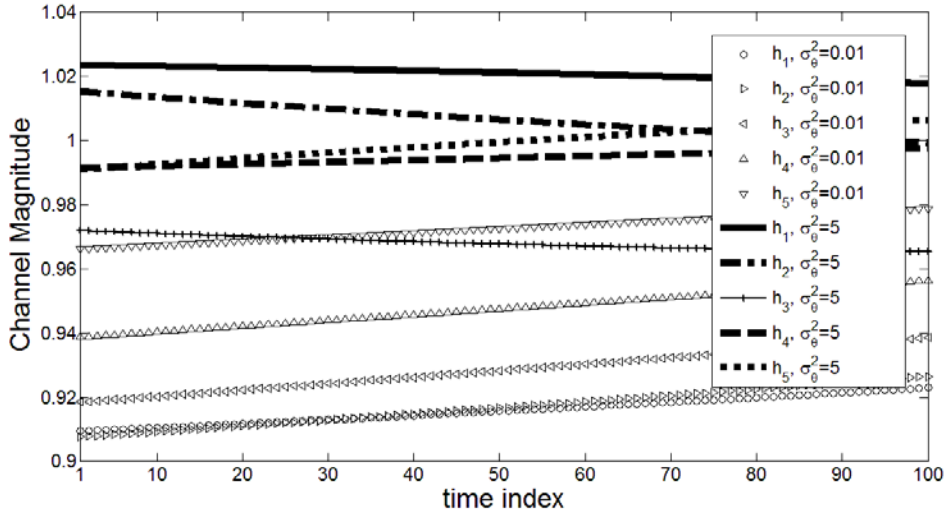

Figure 4. Time domain channel magnitude of first 100 symbols, $N = 5$, $K_R = 25$ dB, $\theta_0 = 30^{\circ}$,$SNR_{elem} = 10$ dB, $F_D T_s = 0.00043$.

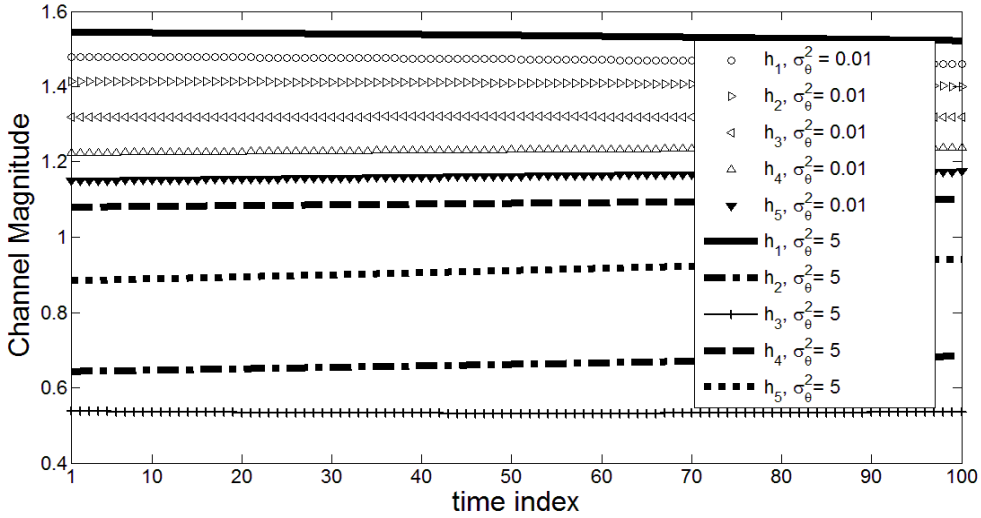

Figure 5. Time domain channel magnitude of first 100 symbols, $N = 5$, $K_R = 10$ dB, $\theta_0 = 30^{\circ}$, $SNR_{elem} = 10$ dB, $F_D T_s = 0.00043$.

The time domain channel magnitude of the first 100 symbols for $K_R = 10$ dB is depicted in Figure 5. The angle spread variance assumed are $\sigma_\theta^2 = 0.01$ and $\sigma_\theta^2 = 5$. In this moderate Rician factor, the angle spread variance influence on the channel elements magnitude is clearly seen. If $\sigma_\theta^2 = 0.01$, the channel is highly correlated, thus the channel elements have similar magnitude if compare to the $\sigma_\theta^2 = 5$ case, where the channel elements magnitude are highly distinct. Nevertheless, during the 100 symbols, the channel magnitude curves can be assumed to stay constant.

respectively.

The upper left part of Figure 7 and 8 illustrate the magnitude of $\boldsymbol{R_{SD}}$ for $\sigma_\theta^2 = 0.01$ and $\sigma_\theta^2 = 5$ respectively. It is seen that as the angle spread σ_θ^2 increases, the shape of the correlation curve is sharper, which means that correlation among different channel pairsisless.

In order to prove our theoretical analysis, i.e. (43) and (52), the estimated autocorrelation matrix $\hat{\boldsymbol{R}}_{\boldsymbol{yy}}$ magnitude for very large, moderate, and very smallRician factors are visualized in Figure 7 and 8. The former is concerned with low angle spread σ_θ^2 = 0.01, whereas the latter with high one $\sigma_\theta^2 = 5$.

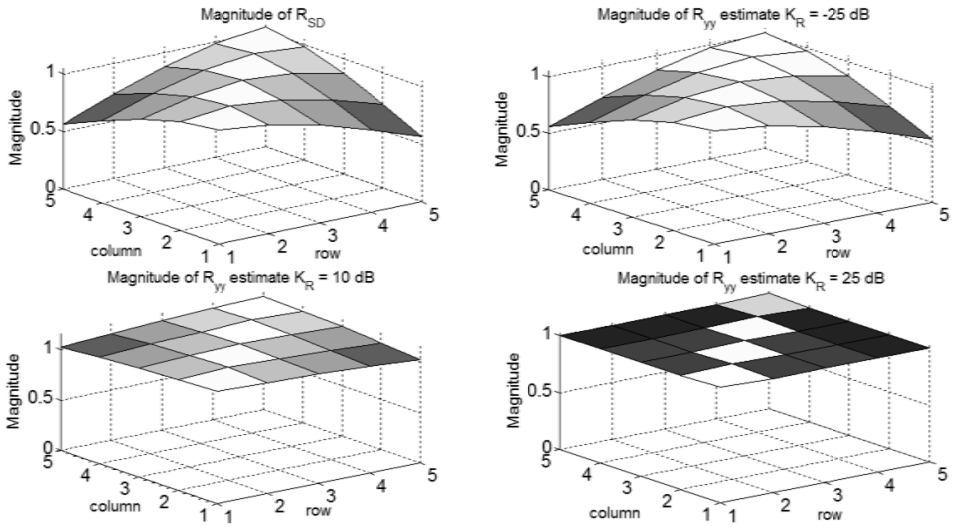

Figure 7. Comparison of R_{SD} and $\hat{\boldsymbol{R}}_{\boldsymbol{yy}}$ magnitude for N = 5,

$\theta_0 = 30^0$, $\sigma_\theta^2 = 0.01$, $\boldsymbol{SNR_{elem}} = 20\boldsymbol{dB}$, $\boldsymbol{F_D T_S} = 0.00043$

There are two results concerning the magnitude of $\hat{\boldsymbol{R}}_{\boldsymbol{yy}}$ for very large Rician factor (K_R = 25 dB) as demonstrated by the bottom right of figure 7 and 8. Firstly, it is observed that both bottom right figures have similar shape, which implies $\hat{\boldsymbol{R}}_{\boldsymbol{yy}}$ is not affected by σ_θ^2. Secondly, both bottom right figures indicate that the magnitude of $\hat{\boldsymbol{R}}_{\boldsymbol{yy}}$ consists of all 1's element. These two observations justify the analysis in (43). In (43), it is seen that $\hat{\boldsymbol{R}}_{\boldsymbol{yy}}$ is independent of σ_θ^2, and its magnitude $\left|\boldsymbol{a}_{\boldsymbol{RX}}^{*}(\theta_0)\,\boldsymbol{a}_{\boldsymbol{RX}}^{T}(\theta_0)\right|$ obviously leads to an all 1's matrix element.

A different observation is found if the Rician factor is moderate (K_R = 10 dB), as visualized in the bottom left of Figure 7 and 8. The shape of both figures are influenced by their respective σ_θ^2 value. If σ_θ^2 is small, the channel becomes highly correlated, thus the magnitude plot of $\hat{\boldsymbol{R}}_{\boldsymbol{yy}}$ in bottom leftof Figure7 produce a fairly smooth curve, as opposed to a peaky shape if σ_θ^2, is high (bottom left of Figure8). Additionally, the $\hat{\boldsymbol{R}}_{\boldsymbol{yy}}$ magnitude if K_R= 10 dB, showed by the bottom left of Figure 7 and 8, resemble closer to the $\hat{\boldsymbol{R}}_{\boldsymbol{yy}}$ of the very large Rician factor case than to R_{SD}.This result is expected since K_R= 10 dB means that the LOS power is 10 times to that of NLOS, such that its $\hat{\boldsymbol{R}}_{\boldsymbol{yy}}$ magnitudeis more influenced by the auto

of the angle spread variance σ_θ^2 employed as statistic parameter of the NLOS component.Consequently, varying the angle spread σ_θ^2doesn't alter the power response. Hence, the solid and dash lines, which represent low and high angle spread variance respectively, coincides.

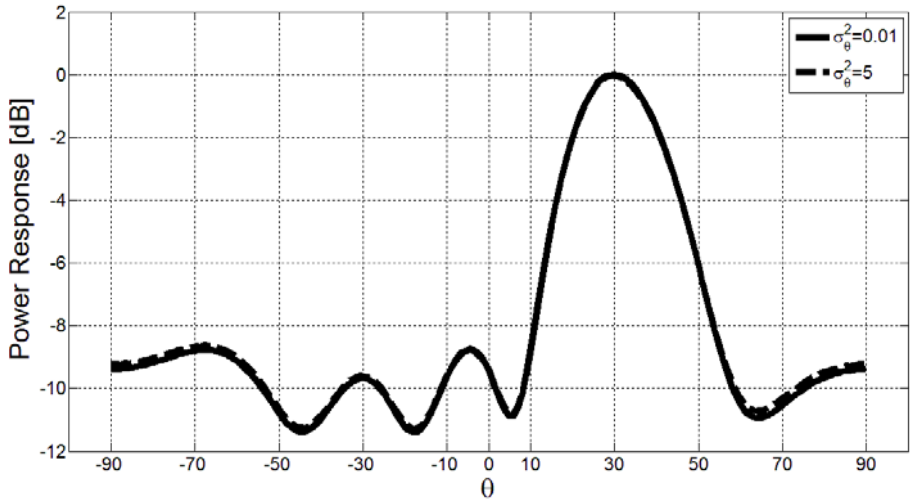

Figure 9. Beamforming weight power response for very largeRician factor, $= 5$, $K_R = 25$ dB, $\theta_0 = 30^\circ$, $SNR_{elem} = 10$ dB, $F_D T_s = 0.00043$

Considering the theoretical analysis of the beamforming weight for very large Rician factor in (46) or (48), the beamforming weight is influenced by both the doppler shift and DOA. Due to the fact that Figure9 plots the power response, only the DOA can be extracted. Its power response can be understood as the power in some angle θ. Since DOA $\theta_0 = 30°$, the power response of (46) or (48) suggest high value. Therefore, the peak at $\theta = 30°$ in Figure9 shows a very good agreement with the theoretical analysis presented in Section 3.
Using (16), the beamforming gain for very large Rician factor and varying angle spread are given as

$$G_{BF}(K_R = 25 \text{ dB}, \sigma_\theta^2 = 0.01) = 3.8084$$

and

$$G_{BF}(K_R = 25 \text{ dB}, \sigma_\theta^2 = 5) = 3.8171$$

The beamforming gain is less than the expected gain which would be obtained from a spatial matched filter, which in a 5 receiver antennas would be$G_{BF} = 5$. The resulting G_{BF} here is limited by the performance of the LS algorithm such that the beamforming weight is not matched perfectly to the channel. Despite this fact, the result of G_{BF} for both $\sigma_\theta^2 = 0.01$ and $\sigma_\theta^2 = 5$ are approximately equal, as is also seen on their respective power response.

C.2. ModerateRician Factor

In order to understand the effect of beamforming weight for varying Rician factors, depicted in Figure10 is the power response for moderate Ricianfactor. The chosen Rician factor is $K_R = 10$ dB.For this value, the channel is affected by both LOS and NLOS components. Accordingly, the power response for $\sigma_\theta^2 = 0.01$ and $\sigma_\theta^2 =$5 are distinguishable.
The beamforming gain for moderate Rician factor and varying angle spread yield

$$G_{BF}(K_R = 10 \text{ dB}, \sigma_\theta^2 = 0.01) = 3.1612$$

and

$$G_{BF}(K_R = 10 \text{ dB}, \sigma_\theta^2 = 5) = 3.9751$$

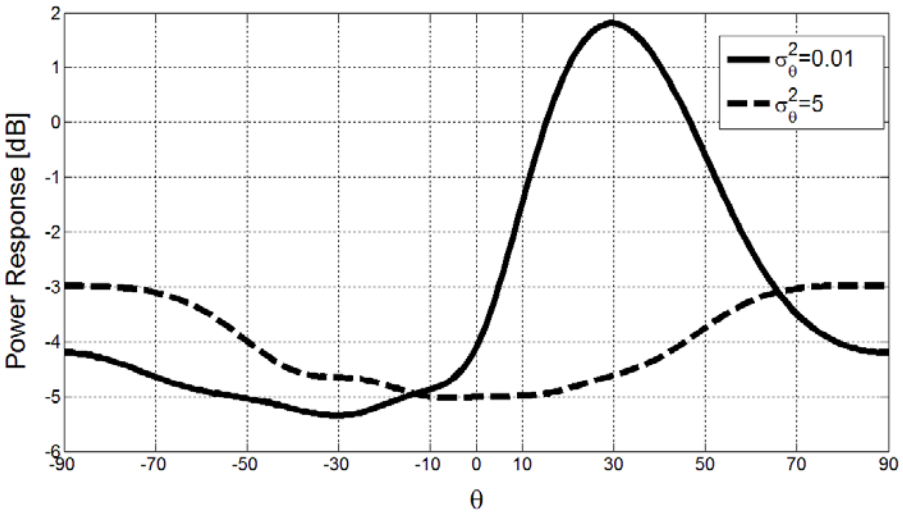

Figure 11. Beamforming weight power response for very small Rician factor,$N = 5$, $K_R = -25$ dB, $\theta_0 = 30^{\circ}$, $SNR_{elem} = 10$dB, $F_D T_s = 0.00043$

We can show that for $F_D T_s = 0.01$, the theoretical analysis of (48), (55), and (56) are also verified by setting a lower number of symbols per frame, i.e. $P = 50$.

5. Summary

Theoretical analysis ofLS beamforming algorithm on the Ka-band channel model of HAP system is given for very large, and additionally, for very small Rician factors, in the high SNR regime. The analysis also considers variation in the angle spread variance of the NLOS channel component. Simulation results verify the theoretical analysis for both the estimated received vector autocorrelation matrix and beamforming weight power response.As the LS performance is influenced by the forgetting factor, it is beneficial to search foralgorithm which determines the forgetting factor based on a certain optimality criteria.Since green communications is desired, future research should consider the low SNR regime analysis and other novel receiver's algorithms with lower complexity than RLS.

6. References

[1] L. Liu, et. al., "Position-Based Modeling for Wireless Channel on High Speed Railway under a Viaduct at 2.35 GHz", *IEEE Journal on Selected Areas in Communications*, vol. 30,. No. 4, 2012.

[2] Cheng Tao, et. al., "Performance Analysis of Doppler Diversity Based on Sectorised Antenna in High-Speed Railway Communication", *Proceedings of IEEE Globecom*, Dec. 2010

[3] M. Aguado, E. Jacob, M. V. Higuero, M. Berbineau and P. Saiz,"Broadband Communication in the High Mobility Scenario: the WiMAX Opportunity," in *WIMAX New Developments*, U. D. Dalal and Y. P. Kosta, Ed., InTech, 2009. Available from: http://www.intechopen.com/books/wimax-new-developments/broadband-communication-in-the-high-mobility-scenario-the-wimax-opportunity

[4] G. Whiteet. al., "Report on adaptive beamforming algorithms for advanced antenna types for aerial platform and ground terminals," FP6 CAPANINA Project, Doc Ref: CAP-D17-WP3.3-UOY-PUB-01 www.capanina.org/documents/CAP-D17-WP3.3-UOY-PUB-01.pdf, Jan. 2006.

[5] G. P. White and Y. V. Zakharov, "Data Communications to Trains FromHigh-Altitude Platforms", IEEE Transactions On Vehicular Technology vol. 56, no. 4, July 2007.

Programs on Telecommunication Engineering at ITB. He has also been actively involved in various collaboration activities with various centres in different countries, such as in European countries (TU Delft The Netherlands, Aalborg University Denmark, Unversity of Duisburg Essen Germany).He has been actively involved in Asia Link EAGER NETWIC that involves 6 universities from Asia and Europe, he was also actively involved in Erasmus Mundus Cooperation Window Mobility for Life that involves 19 universities from Asia and Europe. His current research interests include: Communication Signal Processing, Wireless Communication Systems, and Speech Coding. Dr. Suhartono Tjondronegoro is a member of IEEE-Communication Society. He can be reached through shtntjnegoro@stei.itb.ac.id or shtntjnegoro@gmail.com

Iskandar completed his B.E. and M.E. degrees all in communications engineering from Institut Teknologi Bandung (ITB), Indonesia in 1995 and 2000, respectively. In March 2007, he received his Ph.D. degree from the Graduate School of Global Information and Telecommunication Studies (GITS), Waseda University, Japan. Since April 1997, he joined the Department of Electrical Engineering, ITB, as lecturer. His major research interests are in the areas of radio propagation, channel modelling, mobile communication, stratospheric platform, and millimetre wave band.

A. Kurniawan received B. Eng. in Electrical Engineering from Bandung Institut of Technology, Indonesia, in 1986. He then received M. Eng. and Ph.D in Telecommunication Engineering from the RMIT University and the University of South Australia, respectively in 1996 and 2003. He is currently Associate Professor at School of Electrical Engineering and Informatics, Bandung Institute of Technology, Indonesia. His research interestscovers the area of Antenna and Wave Propagation, and Wireless Communications.